Free convection along a vertical heated plate in a porous medium with anisotropic permeability

P. Vasseur and G. Degan

Department of Mechanical Engineering, Ecole Polytechnique, University of Montreal, Montreal, Canada

Nomenclature

A = aspect ratio of the numerical domain, H/L
a,b,c = constants, equation (8)
c_p = specific heat
f = nondimensional stream function, equation (16)
g = acceleration due to gravity
H = height of the numerical domain
k = thermal conductivity of the saturated porous medium
$\overline{\overline{K}}$ = flow permeability tensor, defined in equation (4)
K_1, K_2 = flow permeability along the principal axes
K^* = permeability ratio, K_1/K_2
L = thickness of the numerical domain
N_{u_x} = local Nusselt number, equation (26)
p = pressure
q = uniform wall heat flux
R_H = Rayleigh number, $K_1 g\beta\Delta TH/\alpha\nu$
R_x = local Rayleigh number, $K_1 g\beta(T_w - T_\infty)x/\alpha\nu$
t = time
T = temperature
ΔT = characteristic temperature difference
$\vec{V}$ = seepage velocity
u,v = velocity components in x and y directions
x,y = cartesian co-ordinates

Greek symbols

α = thermal diffusivity
β = coefficient of thermal expansion of the fluid
θ = inclination of the principal axes
η = similarity variable, equation (18)
Φ = dimensionless temperature
μ = dynamic viscosity of the fluid
ν = kinematic viscosity of the fluid
ρ = density of the fluid
$(\rho c_p)_f$ = heat capacity of the fluid
$(\rho cp)_p$ = heat capacity of the saturated porous medium
λ = exponent in the variation of plate temperature
σ = heat capacity ratio, $(\rho c_p)_p/(\rho c_p)_f$
ψ = stream function

Superscripts

$*$ = dimensionless quantities, equation (32)
$'$ = partial derivative with respect to η

Subscripts

ω = vertical boundary (wall)
∞ = distance far from the vertical boundary

Note: The symbols defined above are subject to alteration on occasion

Introduction

Natural convection heat transfer from a vertical plate embedded in a fluid saturated porous medium is of great practical importance in many branches of engineering. Applications include petroleum and geothermal industries, the storage of radioactive nuclear materials, ground water pollution, etc. In a

This work was supported in part by the Natural Sciences and Engineering Research Council, Canada and jointly by the FCAR, Government of Quebec.

International Journal for Numerical Methods for Heat & Fluid Flow
Vol. 8 No. 1, 1998, pp. 43–63.

review article, Cheng (1978) has discussed various works done in this field as applied to geothermal systems.

Cheng and Minkowycz (1977) treated buoyancy induced flows over a semi-infinite flat plate in a porous medium. Under the boundary-layer and Darcy's approximations, similarity solutions were obtained for the case of a surface with prescribed wall temperature. A systematic analysis, regarding the possibility of similarity solutions for various wall temperature functions, was undertaken by Johnson and Cheng (1978). Seetharamu and Dutta (1990) considered the problem of a vertical plate with wall temperature varying as an arbitrary function of the distance from the origin. Nakayama and Koyama (1987) used an integral procedure for the analysis of free convection from a vertical heated surface in a thermally stratified porous medium. Effects of the thermal stratification on local heat transfer rates was discussed. A finite element analysis of convection past a vertical surface embedded in a porous medium was performed by Rajamani *et al.* (1990). In their study, the restriction of the boundary-layer assumption was relaxed. The transient free convection flow in a saturated porous medium near a vertical flat impermeable surface which is suddenly cooled to the same temperature as the ambient fluid has been considered by Ingham *et al.* (1982). Analytical solutions for small and large time were derived by these authors.

A few studies have also been reported for the case of a vertical plate on which the variation of heat flux is specified instead of the wall temperature, since such a condition is encountered in some practical applications. Free convection from a vertical plate with uniform heat flux has been discussed by Cheng (1977). The problem was reconsidered by Dutta and Seetharamu (1987, 1993) for a heat flux varying as power function from the origin as well as for a non-uniform heat flux. Several investigations have been undertaken to take into account the boundary and inertia effects, not included in Darcy's model, which may become important in high permeability media. Evans and Plumb (1978) and Hsu and Cheng (1985) studied the boundary friction effect on heat transfer based on Brinkman's equation. Plumb and Huenefeld (1981), Bejan and Poulikakos (1984) used Forschheimer's equation to account for the influence of a quadratic drag on natural convection over a vertical surface. Hong *et al.* (1985) and Seetharamu *et al.* (1994) considered both the boundary and inertia effects as well as the convective term in their model to investigate the significance of these effects on natural convection in a high-porosity medium. Kaviany and Mittal (1987) studied both analytically and experimentally the heat transfer rate from an isothermal vertical plate placed next to a high permeability porous medium. It was demonstrated by these investigators that both the boundary and inertia effects decrease the heat transfer rate.

In all the above studies the porous media were assumed to be isotropic whereas, in several applications, the porous materials are anisotropic. Despite this fact, natural convection in such anisotropic porous media has received relatively little attention. The effects of an anisotropic permeability on thermal convection in a porous medium began with the investigation of Castinel and

Combarnous (1974), concerning the onset of motion in a horizontal layer heated from below, and continued with the works of Epherre (1975), Kvernvold and Tyvand (1979) and Nilsen and Storesletten (1990). Natural convection within enclosures heated from the side was investigated by Kimura *et al.* (1993) and Ni and Beckermann (1991), for the case when one of the principal axes of anisotropy of permeability is aligned with gravity and by Zhang (1993), Degan *et al.* (1995) and Degan and Vasseur (1996) when the principal axes are inclined with respect to gravity. It was demonstrated by these authors that the effects of the anisotropy considerably modify the convective heat transfer. Recently, the effects of anisotropy on the boundary-layer free convection over an impermeable vertical plate, for the case when one of the principal axes of anisotropy is along the plate, were investigated by Ene (1991), using the method of integral relations. It was concluded that, if the permeability in the direction normal to the plate is greater than the permeability along the plate, then there is an increase in the temperature field.

The present work is devoted to the study of natural convection over a vertical heated plate adjacent to a porous medium. This latter is anisotropic in permeability with its principal axes oriented in a direction that is oblique to the gravity vector. Within the framework of boundary-layer approximations, similarity solutions are obtained for the case where wall temperature varies as a power function of distance from the leading edge. The full governing equations are solved numerically, using a finite-difference procedure. Effects of governing parameters, namely the Rayleigh number R, the permeability ratio K^* and the angular position θ of the principal axes on local heat transfer rates are discussed.

Mathematical formulation

We consider the problem of steady heating of a vertical flat plate embedded in a saturated porous medium characterized by an anisotropic permeability. The x and y axes are aligned with the vertical and the horizontal respectively as shown in Figure 1a. The permeabilities along the two principal axes of the porous matrix are denoted by K_1 and K_2. The anisotropy of the porous medium is characterized by the anisotropy ratio $K^* = K_1/K_2$ and the orientation angle θ, defined as the angle between the horizontal direction and the principal axis with permeability K_2.

The convective fluid and the porous medium are assumed to be everywhere in local thermodynamic equilibrium. The thermophysical properties of the fluid are taken constant, except for the density in the buoyancy term in the momentum equation. Under these assumptions, the Darcy system of equations describing the convective, laminar, two-dimensional, incompressible flow in an anisotropic porous medium can be written as follows (Bear, 1972)

$$\nabla.\vec{V} = 0 \tag{1}$$

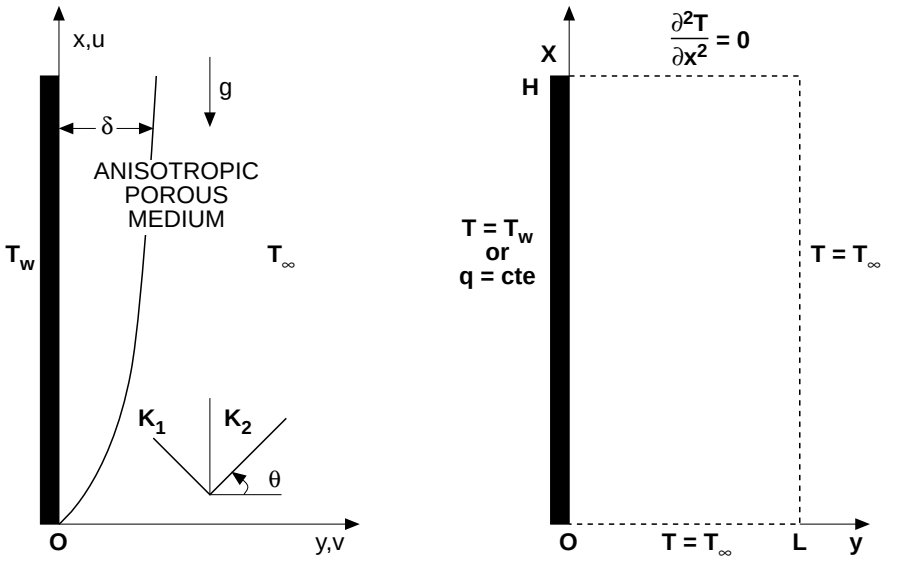

Figure 1.
(a) Physical model and co-ordinates; (b) numerical domain

$$\vec{V} = \frac{\overline{\overline{K}}}{\mu}\left(-\nabla p + \varrho \vec{g}\right) \tag{2}$$

$$\sigma\frac{\partial T}{\partial t} + \nabla.\left(\vec{V}\,T\right) = \alpha\,\nabla^2 T \tag{3}$$

where $\vec{V}$ is the Darcian velocity, ρ the density, μ the viscosity, p the pressure, T the temperature, t the time, $\vec{g}$ the gravitational acceleration, σ the heat capacity ratio of the fluid-filled porous medium to that of the fluid and α the equivalent thermal diffusivity of the porous medium. The second-order permeability tensor $\overline{\overline{K}}$ is defined as

$$\overline{\overline{K}}' = \begin{bmatrix} K_1\cos^2\theta + K_2\sin^2\theta & (K_1 - K_2)\sin\theta\cos\theta \\ (K_1 - K_2)\sin\theta\cos\theta & K_2\cos^2\theta + K_1\sin^2\theta \end{bmatrix} \tag{4}$$

Introducing the Boussinesq approximation

$$\varrho = \varrho_o[1 - \beta(T - T_o)] \tag{5}$$

where β is the thermal expansion coefficient of the fluid and ρ_0 and T_0 are the density and temperature of the fluid at a reference condition and eliminating the

pressure term in the momentum equation in the usual way, the governing equations become

$$a\frac{\partial^2\psi}{\partial y^2} + b\frac{\partial^2\psi}{\partial x\partial y} + c\frac{\partial^2\psi}{\partial x^2} = \frac{K_1 g\beta}{\mu}\frac{\partial T}{\partial y} \tag{6}$$

$$\sigma\frac{\partial T}{\partial t} + \frac{\partial\psi}{\partial y}\frac{\partial T}{\partial x} - \frac{\partial\psi}{\partial x}\frac{\partial T}{\partial y} = \alpha\nabla^2 T \tag{7}$$

where

$$\left.\begin{aligned} a &= \cos^2\theta + K^*\sin^2\theta \\ b &= 2(K^*-1)\sin\theta\cos\theta \\ c &= \sin^2\theta + K^*\cos^2\theta \end{aligned}\right\} \tag{8}$$

In the above equations ψ is the stream function related to the velocity components by

$$u = \frac{\partial\psi}{\partial y}, \qquad v = -\frac{\partial\psi}{\partial x} \tag{9}$$

such that the continuity equation (1) is automatically satisfied.

In the following sections the above equations will be solved both analytically, under the boundary-layer approximations, and numerically, considering the full set of governing equations. The boundary conditions pertinent to each of those two situations will then be specified.

Boundary-layer solution

The boundary-layer problem is considered first. From the momentum equation (6) it is clear that a boundary-layer regime is possible only when the second and the third terms, on the left-hand side of the equation, can be neglected when compared with the first one, i.e. when the conditions $a\psi_{yy} \gg b\psi_{xy}$ and $a\psi_{yy} \gg c\psi_{xx}$ are satisfied. Taking δ as the thickness of the boundary-layer and assuming that $x \sim H$, $y \sim \delta$, $\psi \sim \alpha H/\delta$ and $T \sim 1$, see for instance Ene and Polisevski (1987), it follows that the conditions

$$\frac{a}{b}\frac{H}{\delta} \gg 1 \tag{10}$$

and

$$\frac{a}{c}\frac{H^2}{\delta^2} \gg 1 \tag{11}$$

must be satisfied.

Equations (10) and (11) indicate that, if $a/b = O(1)$ and $a/c = O(\delta/H)$, the boundary-layer hypothesis can be used. However, if $a/b = O(\delta/H)$ and $a/c = O(\delta^2/H^2)$, then the terms on the left hand side of equation (6) are of the same order of magnitude and the boundary-layer approximations cannot be involved.

In the boundary-layer regime, i.e. when conditions (10) and (11) are satisfied, it can be readily demonstrated that equations (6) and (7), for a steady state regime, reduce to

$$a\,\frac{\partial^2\psi}{\partial y^2} = \frac{K_1 g\beta}{\mu}\,\frac{\partial T}{\partial y} \tag{12}$$

$$\frac{\partial^2 T}{\partial y^2} = \frac{1}{\alpha}\left(\frac{\partial\psi}{\partial y}\,\frac{\partial T}{\partial x} - \frac{\partial\psi}{\partial x}\,\frac{\partial T}{\partial y}\right) \tag{13}$$

For the co-ordinate system shown in Figure 1a the boundary conditions prevailing on the wall and at great distance from the wall are

$$y = 0: \qquad \frac{\partial\psi}{\partial x} = 0, \qquad T = T_w = T_\infty + Cx^\lambda \tag{14}$$

$$y \to \infty: \qquad \frac{\partial\psi}{\partial y} = 0, \qquad T = T_\infty \tag{15}$$

where the prescribed wall temperature T_w is a power function of distance x, C is a constant and T_∞ is the temperature in the porous medium far away from the wall.

We now introduce the following transformations

$$\psi = \alpha\left(\frac{R_x}{a}\right) f(\eta) \tag{16}$$

$$\Phi(\eta) = (T - T_\infty)/(T_w - T_\infty) \tag{17}$$

$$\eta = \frac{y}{x}\left(\frac{R_x}{a}\right)^{1/2} \tag{18}$$

where

$$R_x = \frac{K_1 g\beta(T_w - T_\infty)\,x}{\alpha\mu} \tag{19}$$

is the local Rayleigh number while η is the similarity parameter. The substitution of equations (16)-(18) into equations (12) and (13) yields

$$f'' - \Phi = 0 \tag{20}$$

$$\Phi'' + \frac{(1+\lambda)}{2} f\Phi' - \lambda f'\Phi = 0 \tag{21}$$

with the boundary conditions given by

$$\eta = 0: \qquad f = 0, \qquad \Phi = 1 \tag{22}$$

$$\eta \to \infty: \qquad f' = 0, \qquad \Phi = 0 \tag{23}$$

The primes in the above equations denote the derivatives with respect to η. In terms of the similarity variable η, the seepage velocity components are

$$u = \frac{\alpha}{x} \frac{R_x}{a} f'(\eta) \tag{24}$$

$$v = \frac{\alpha}{2x} \left(\frac{R_x}{a}\right)^{1/2} [(1-\lambda)\eta f' - (1+\lambda) f] \tag{25}$$

The local Nusselt number Nu_x is defined as

$$Nu_x = \frac{h\,x}{k} \tag{26}$$

where $h = q/(T_w - T_\infty)$ is the local heat transfer coefficient and $q = -k\,(\partial T/\partial y)_{y=0}$ the local surface heat flux at the heated plate. In terms of the similarity parameters, equations (16)-(18), it is readily found that

$$Nu_x = \left(\frac{R_x}{a}\right)^{1/2} [-\Phi'(0)] \tag{27}$$

Equations (20) and (21), subjected to boundary conditions (22) and (23), are similar to those obtained by Cheng and Minkowycz (1977) while studying free convection about a vertical plate embedded in an isotropic porous medium ($K^* = 1$). Integration of these equations were performed by these authors, for different values of λ, using a standard numerical procedure. Of special interest for the present study are the results $[-\Phi'(0)] = 0.444$ and $[-\Phi'(0)] = 0.6788$, in equation (27), obtained for the case of an isothermal surface ($\lambda = 0$) and a constant flux surface ($\lambda = 1/3$) respectively.

The size of the porous layer δ, where the effect of the presence of wall is felt, can now be estimated. Let η_δ be the value at the edge of the boundary-layer, i.e. at $y = \delta$, where Φ is equal to 0.01 it is found from equation (18) that

$$\frac{\delta}{x} = \eta_\delta \left(\frac{R_x}{a}\right)^{-1/2} \tag{28}$$

where, according to Cheng and Minkowycz (1977), $\eta\delta$ = 6.31 and 5.50 for the case of an isothermal and a constant flux surface respectively. Thus, the conditions for the validity of the present boundary-layer solution can be estimated from equations (10), (11) and (28).

Numerical procedure

The numerical simulations in this study were performed based on the complete form of the governing equations. In dimensionless form, equations (6) and (7) can be rewritten as

$$a\frac{\partial^2\psi^*}{\partial y^{*2}} + b\frac{\partial^2\psi^*}{\partial x^*\partial y^*} + c\frac{\partial^2\psi^*}{\partial x^{*2}} = R_H\frac{\partial T^*}{\partial y^*} \tag{29}$$

$$\frac{\partial T^*}{\partial t^*} + u^*\frac{\partial T^*}{\partial x^*} + v^*\frac{\partial T^*}{\partial y^*} = \nabla^2 T^* \tag{30}$$

where

$$R_H = \frac{K_1 g\beta\Delta T H}{\alpha\mu} \tag{31}$$

is the Rayleigh number based on the height H of the heated plate.

The nondimensionalization was carried out according to the following definitions

$$\left.\begin{aligned} (x^*, y^*) &= \frac{(x,y)}{H} & (u^*, v^*) &= \frac{(u,v)H}{\alpha} & \psi^* &= \frac{\psi}{\alpha} \\ T^* &= \frac{T - T_\infty}{\Delta T} & t^* &= \frac{t\,\alpha}{\sigma H^2} \end{aligned}\right\} \tag{32}$$

where ΔT is a characteristic temperature difference which depends on the thermal boundary conditions applied on the plate. Thus, when the plate is maintained at a constant temperature T_w, $\Delta T = T_w - T_\infty$ while, when the plate is heated by a uniform heat flux q (per unit area), $\Delta T = qH/k$. Both cases will be considered in the numerical simulations.

Following Mahajan and Angirasa (1993), the dimensionless boundary conditions applied on the computational domain shown in Figure 1b are

$$
\left.
\begin{array}{llll}
x^* = 0: & \dfrac{\partial \psi^*}{\partial x^*} = 0, & T^* = 0 & \\
x^* = 1: & \dfrac{\partial \psi^*}{\partial x^*} = 0, & \dfrac{\partial^2 T^*}{\partial x^{*2}} = 0 & \\
y^* = 0: & \psi^* = 0, & T^* = 1 & \text{wall at a constant temperature} \\
 & & \dfrac{\partial T^*}{\partial y^*} = -1 & \text{wall with uniform heat flux} \\
y^* = A: & \dfrac{\partial \psi^*}{\partial y^*} = 0, & T^* = 0 &
\end{array}
\right\} \quad (33)
$$

where $A = L/H$ is the aspect ratio of the rectangular numerical domain. The imposition of a second-order derivative on the temperature at $x^* = 1$, equation (33), is similar to the approach used in the past by Yücel *et al.* (1993).

The local Nusselt number, based on the height of the plate, is given, according to equation (26), by $Nu_H = hH/k$. It follows that, in the case of a plate maintained at a constant temperature, one obtains

$$Nu_H(x^*) = -\left.\frac{\partial T^*(x^*)}{\partial y^*}\right|_{y^*=0} \quad (34)$$

while for the case of a plate heated by a constant heat flux the local Nusselt number is given by

$$Nu_H(x^*) = \frac{1}{T_w^*(x^*)} \quad (35)$$

where $T_w^*(x^*)$ is the local dimensionless temperature of the wall.

The energy equation (30) was solved numerically using the well-known alternating direction implicit (ADI) scheme of Peaceman (Roache, 1982). The temporal and spatial derivatives are approximated by first and second-order discretizations respectively. A successive over relaxation (SOR) method was employed for the solution of the stream function (29). The following criteria were used to check convergence of all variables at all nodal points

$$\frac{\sum_i \sum_j \left|\Omega_{i,j}^{new} - \Omega_{i,j}^{old}\right|}{\sum_i \sum_j \left|\Omega_{i,j}^{new}\right|} \leq \Gamma \quad (36)$$

where Ω is T and ψ, i and j refer to space and Γ is a constant, usually set to 10^{-4} or less. A second-order forward and backward discretization is carried out to approximate the hydrodynamic and thermal boundary conditions imposed on the physical domain.

Based on several trial cases the aspect ratio of the computational domain was chosen to be $A = 0.25$. This value was estimated from the similarity solutions and it was verified that higher values did not alter the solution significantly. For the present work, uniform mesh sizes have been used for both x– and y–directions. A grid field of (40×60) was used for most of the calculations reported in this study. In the cases where a very thin boundary-layer along the heated plate was observed, the grid fineness was improved up to 100×120. Typical values of the time steps range from 10^{-3} to 5×10^{-5}.

Results and discussion

The isotropic porous medium

To test the validity of the algorithm, the numerical results were first compared with the boundary-layer solution of Cheng and Minkowycz (1977) for the case of an isotropic porous medium ($K^* = 1$).

The local Nusselt number $Nu_z/(R_x)^{1/2}$ is plotted in Figure 2a as a function of the Rayleigh number R_H, based on the height of the plate. The symbols represent the results of numerical solution, obtained at mid-height of the plate ($x^* = 0.5$), both for the case of a wall heated isothermally and by a uniform flux. The analytical results $Nu_x/(R_x)^{1/2} = 0.444$ (isothermal) and 0.678 (constant flux), predicted by Cheng and Minkowycz (1977) on the basis of the boundary-layer approximations, are also indicated on the graph for comparison. For very large values of R_H, i.e. in the boundary-layer regime, the agreement between the analytical and the numerical results is observed to be excellent. On decreasing R_H it is seen that the boundary-layer regime can be maintained up to a given Rayleigh number under which the heat transfer rate predicted by Cheng and Minkowycz's similarity solution becomes invalid. The breakdown of the boundary-layer approximation occurs at $R_H \simeq 10^2$ for the plate heated isothermally and $R_H \simeq 10^3$ for the plate with uniform heat flux. As R_H is further reduced the local Nusselt number Nu_x decreases steadily ($Nu_x/(R^x)^{1/2}$ increases) since the strength of the convective flow along the flat plate becomes weaker. It is well know that the similarity character of the boundary-layer equations describing natural convection over a vertical plate is applicable only far from the leading edge. This point is illustrated in Figure 2b where the local Nusselt number Nu_x is plotted as a function of x^*, the dimensionless position along the vertical plate. The numerical results were obtained for $R_H = 10^3$ and 2×10^3 for which a boundary-layer regime prevails. The parameter $Nu_x/(R_x)^{1/2}$ is observed to increase from zero at the origin of the space co-ordinates ($x^* = 0$), up to a maximum value located near the leading edge of the plate, and then decreases monotonously towards the constant values reported by Cheng and Minkowycz (1977). The similarity solutions are seen to be valid at a distance $x^* \simeq 0.2$ for an isothermal plate and $x^* \simeq 0.4$ for a uniform heat flux surface. For this reason, in

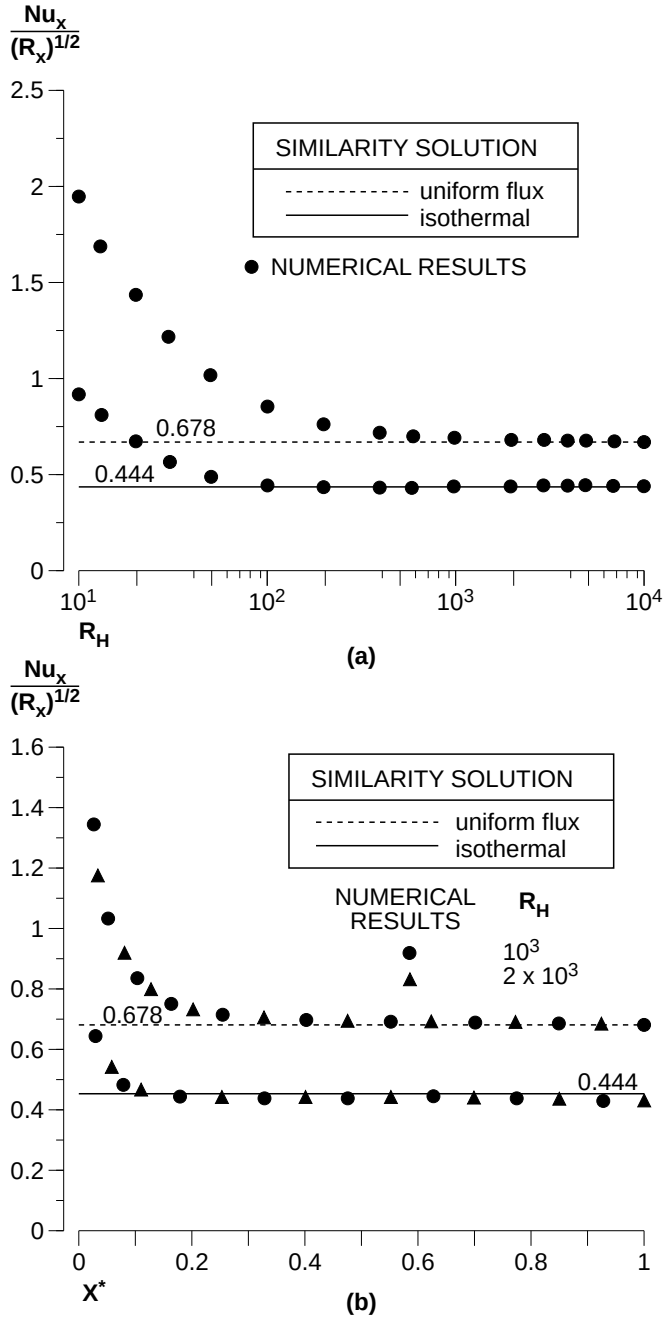

Figure 2.
(a) Variation of $Nu_x/(R_x)^{1/2}$ versus x^*; (b) variation of $Nu_x/(R_x)^{1/2}$ at mid-height of the plate versus R_H.

the following section, the analytical solutions concerning the anisotropic porous medium are compared with the numerical results obtained at the arbitrary position $x^* \simeq 0.5$ Such a distance is far enough from the leading edge to insure the similarity character of the boundary-layer solution.

Figure 3 shows the dimensionless temperature Φ and velocity distribution f', at mid-height of the plate ($x^* = 0.5$), versus the similarity variable η. The computed values obtained for $R_H = 3 \times 10^3$ and 5×10^3 are seen to be in good agreement with the similarity solutions of Cheng and Minkowycz (1977), the maximum difference between the two solutions being less than about 1.5 per cent. Having gained confidence in the validity of the numerical code, this latter will be now used to investigate the effects of anisotropy in permeability on the present problem.

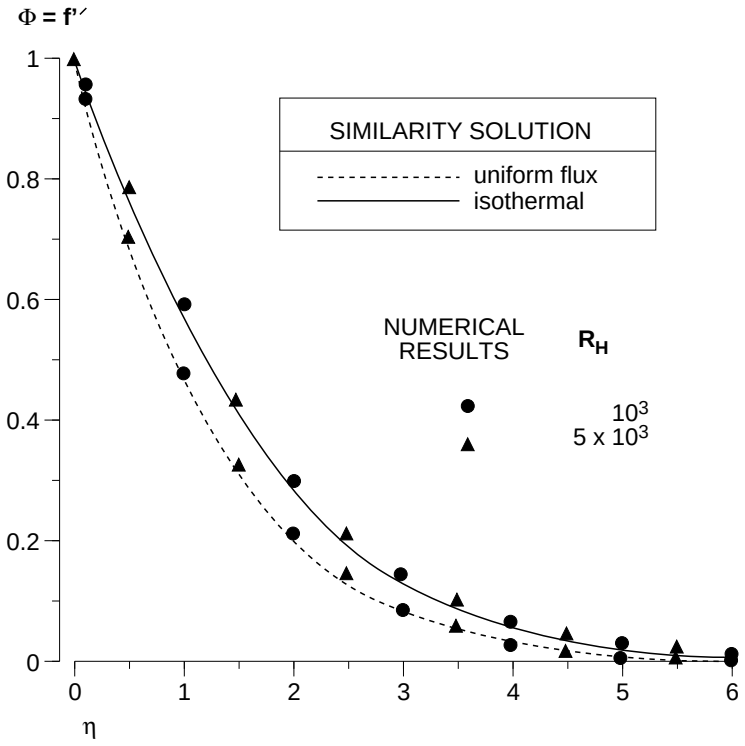

Figure 3.
Dimensionless temperature Φ and vertical velocity f' versus the similarity variable η.

The anisotropic porous medium

In this section the effects of the permeability ratio K^* and the angular position θ of the principle axes, on the free convection over a vertical plate, will be discussed both for the isothermal and the constant heat flux situations.

Figure 4a-c shows typical numerical results illustrating the effects of the orientation angle θ on the streamlines (left) and isotherms (right) along an

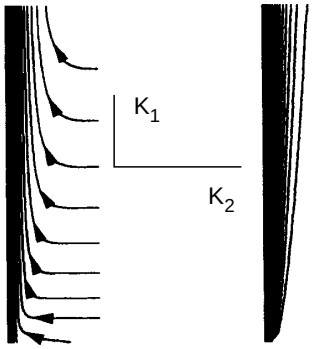

(a)

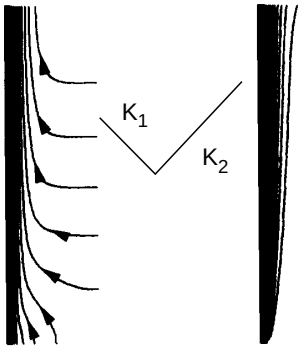

(b)

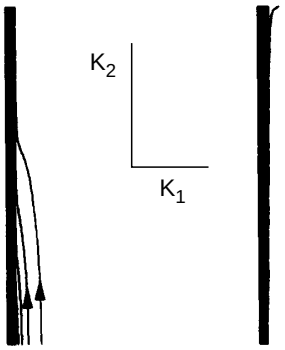

(c)

Figure 4.
Numerical solutions for the flow and temperature fields for the case of an isothermal plate embedded in an anisotropic porous medium for $R_H = 10^3$, $K^* = 10^{-2}$; (a) $\theta = 0°$, $\psi_{max} = 50.515$; (b) $\theta = 45°$ $\psi_{max} = 67.864$; (c) $\theta = 90°$, $\psi^{max} = 526.96$.

isothermal plate for $R_H = 10^3$ and $K^* = 10^{-2}$ (i.e. $K_1 < K^2$). In those graphs the increments between adjacent streamlines and isotherms are $\Delta\psi = \psi_{max}/10$ and $\Delta T = 0.1$, where ψ_{max} is the maximum value of the stream function. For convenience, the direction and relative importance of the maximum and minimum permeabilities are depicted by the angular position and relative lengths of the perpendicular lines located between each set of flow and temperature fields. The results obtained for $\theta = 0°$, i.e. when the minimum (maximum) permeability of the porous medium is along (perpendicular) the plate, are depicted in Figure 4a. The fluid nearest to the plate warms up, decreases its density and moves upwards according to Archimede's law. The formation of a thin boundary-layer along the plate, in which the fluid flows essentially upwards, is clearly observed. Because of continuity the fluid outflow from this area causes an influx of fluid from the side, which is seen to move essentially in the horizontal direction. This flow pattern is similar to what would be observed for the isotropic case ($K^* = 1$). The effects of the anisotropy orientation on the flow and temperature patterns are depicted in Figures 4b and c for $\theta = 45°$ and 90° respectively. In general, the strength of the convective flow, as indicated by the value of ψ_{max}, is enhanced as the orientation of the principal axis with higher permeability is changed from horizontal ($\theta = 0°$) to vertical ($\theta = 90°$). The anisotropy orientation θ is also observed to have an important influence on the flow field. Thus, when $\theta = 45°$, Figure 4b indicates that the fluid outside the boundary-layer flows not only from the side, as in Figure 4a for $\theta = 0°$, but also from below the plate in the vicinity of the leading edge. This tendency is more pronounced as the orientation anisotropy θ is increased from 45° to 90°. For this situation, the permeability in the vertical direction is much greater than the permeability in the horizontal direction ($K_2 \gg K_1$) such that the flow is essentially channeled along the plate.

Figure 5a shows the distribution of the vertical velocity u^*, at mid-height of an isothermal plate, for a porous medium with a permeability ratio $K^* = 0.25$ (i.e. $K_2 > K_1$) and different orientation angle θ, as predicted by the present boundary-layer analysis. The blackened symbols in this graph are the results of the numerical simulation, for $R_H = 2 \times 10^3$ and 4×10^3, which are seen to be in good agreement with the analytical solution represented as solid lines. The graph indicates that the velocity is maximum at the wall. This is in agreement with the fact that the porous medium has been modeled according to Darcy's law such that the fluid is allowed to slip on the solid boundary. It is seen from Figure 5a that the magnitude of the vertical velocity is greatly affected by the orientation angle θ. Thus, as expected, the velocity at the side wall is larger (smaller) for $\theta = 90°$ ($\theta = 0°$), i.e. when the maximum (minimum) permeability is oriented in the direction of the boundary-layer flow along the plate. For intermediate values of θ the velocity at the wall has a magnitude included between these two extreme values, as exemplified by the curve for $\theta = 45°$. The

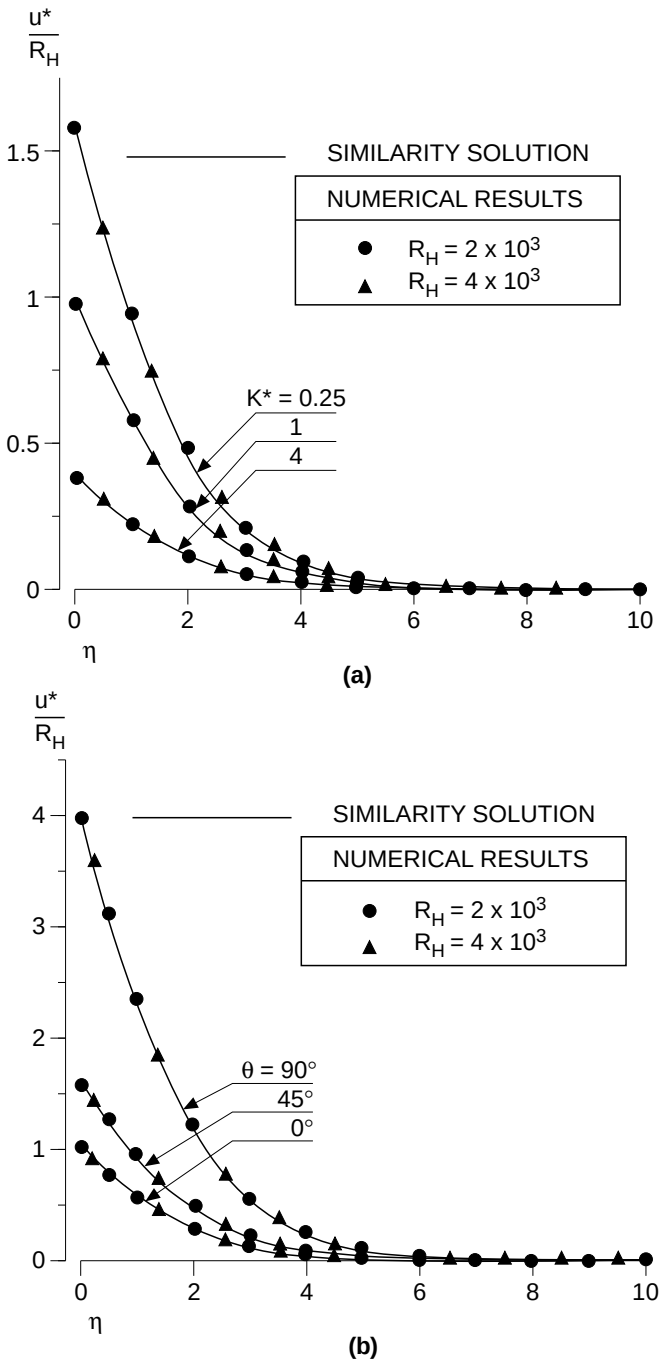

Figure 5.
Vertical velocity at u^*, at mid-height of an isothermal plate, for various values of (a) the anisotropy ratio K^*; (b) the inclination angle θ.

fact that the flow in an anisotropic porous medium is maximum when the orientation of the principal axis with higher permeability is parallel to the gravity while it is minimum when it is perpendicular to this latter has already been reported in the past by Zhang (1993) and Degan *et al.* (1995) and Degan and Vasseur (1996) for the case of natural convection within a rectangular cavity heated differentially from the sides. The effect of the permeability ratio K^* on the velocity distribution for a porous medium with an isotropic orientation $\theta = 45°$ is depicted in Figure 5b. The case with $K^* = 1$ corresponds to an isotropic porous medium as considered in the past by Cheng and Minkowycz (1977). For a given Rayleigh number R_H, i.e. a fixed value of K_1, an increase of K^* corresponds to a decrease of K_2 and thus of the strength of the convective flow. Naturally, the reverse effect is observed as the value of K^* is decreased.

Figures 6a and b show the effect of the Rayleigh number R_H on the local Nusselt number Nu_x, at mid-height of an isothermal plate, for various values of θ and $K^* = 4$ and 0.25 respectively. The numerical results indicate that when R_H is large enough, in order for the flow along the plate to be in the boundary-layer regime, the ratio $Nu_x/[0.444(R_x/a)^{1/2}]$ is equal to unity in agreement with the prediction of the analytical solution, equation (27). The value of R_H necessary to reach this regime is seen to depend on both K^* and θ. For instance, when $\theta = 0°$, Figures 6a and b indicate that a boundary-layer regime is reached at about $R_H \simeq 10^3$ when $K^* = 4$ and $R_H \simeq 2 \times 10^2$ when $K^* = 0.25$. For this inclination angle K_1 is oriented along the plate and K_2 is normal to it. In the boundary-layer regime, the flow along the vertical plate results from the horizontal entrainment of the fluid at infinity. It is thus expected that, as the value of K^* is decreased, i.e. the permeability in the direction perpendicular to the plate increased, the flow in the horizontal direction will be enhanced such that a boundary-layer regime can be reached at a smaller R_H. A similar argument applies when $\theta = 90°$ for which the permeability K_2 is now oriented along the plate. For a fixed value of K_1, a decrease of K^* implies an increase of K_2 for which the flow along the plate is promoted such that a boundary-layer regime occurs at a relatively lower value of R_H.

In Figure 7 the local Nusselt number Nu_x, at mid-height of the plate, is given as a function of θ and K^* both for the case of a wall heated isothermally (solid lines) and by a uniform flux (dashed lines). The numerical results obtained for $R_H = 3 \times 10^3$ and 5×10^3 are seen to agree well with the analytical solution. According to equation (27) it is observed that the parameter $Nu_x/(R_x)^{1/2}$ depends on $[\Phi'(0)]a^{-1/2}$, where $[\Phi'(0))]$ is a constant that depends on the heating process and $a = cos^2\theta + K^* sin^2\theta$, i.e. on the anisotropic properties of the porous medium, namely the permeability ratio K^* and the inclination angle θ. The particular cases $\theta = 0°$ and 90°, for which the principal axes of anisotropy are aligned with the gravity vector, will be first discussed. When $\theta = 0°$ ($a = 1$), Figure 7 indicates that the parameter $Nu_x/(R_x)^{1/2}$ is constant, independent of the value of the ratio of the permeabilities K^*. For this situation the local heat transfer, in the boundary-layer regime, depends solely on the Rayleigh number

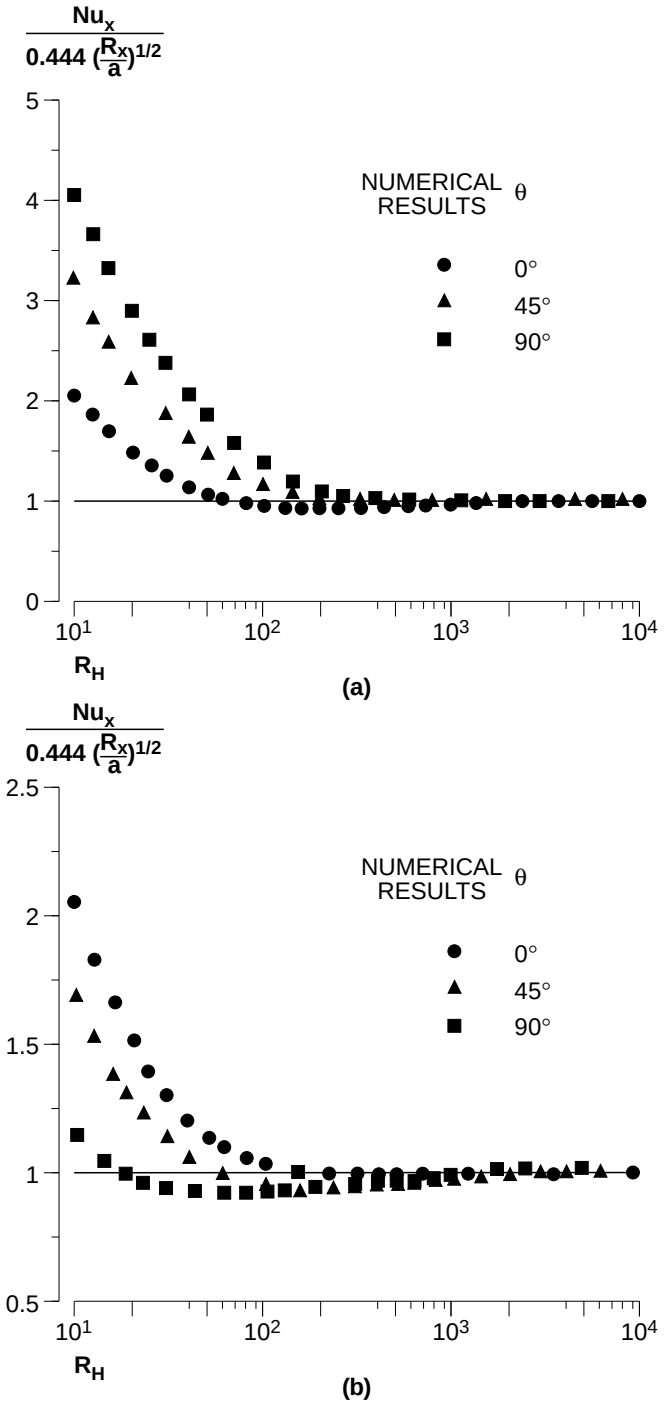

Figure 6.
Variation of the local Nusselt number Nu_x, at mid-height of an isothermal plate versus R_H for (a) $K^* = 4$; (b) $K^* = 0.25$

R_x based on the permeability K_1 along the plate, and is not affected by the magnitude of the permeability K_2 in the direction normal to it. Naturally, as illustrated in Figure 6, the minimum Rayleigh number necessary to reach a boundary-layer flow regime along the flat plate does depend on K_2. For $\theta = 90°$ ($a = K^*$) the permeability K_2 is now aligned along the plate while the permeability K_1 is in a direction orthogonal to it. According to Figure 7, the resulting local Nusselt number depends strongly on the permeability ratio K^*. This trend follows from the fact that R_x, which is based on K_1 the permeability now perpendicular to the plate, is not the appropriate parameter for this situation. Thus, according to equation (27), on using a Rayleigh number $R_x/a = K_2 g\beta\Delta Tx/\alpha\mu$, based on the permeability K_2 along the plate, the local Nusselt number Nu_x becomes independent of K^*. Recently, the effects of anisotropy on the boundary-layer free convection over a vertical impermeable surface has been investigated by Ene (1991). The governing boundary-layer equations were solved, using the method of integral relation, for the case when the principal axes of anisotropy are aligned with the plate. This problem, however, is

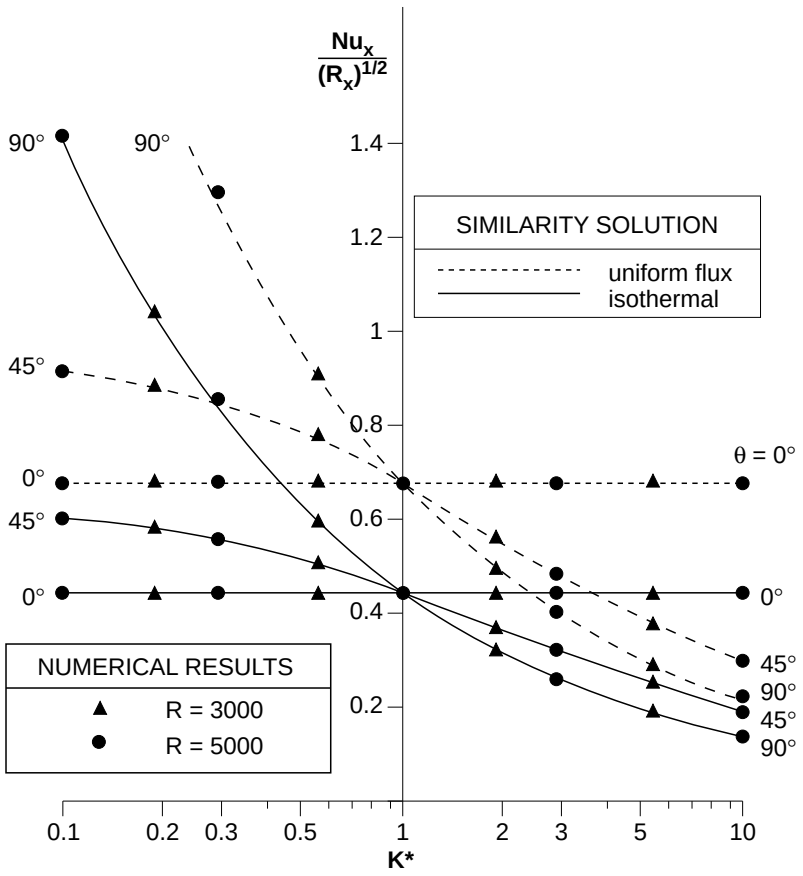

Figure 7.
Variation of the local Nusselt number Nu_x, at mid-height of the plate versus K^* for various values of θ.

marginal since, as discussed above, on using an appropriate normalization the convective heat transfer can be directly deduced from the solution for an isotropic porous situation ($K^* = 1$). For an arbitrary orientation of the inclination angle θ the solution depends strongly on K^*. This point is illustrated in Figure 7 for $\theta = 45°$ for which it is seen that, as the permeability ratio K^* is made larger, the value of Nu_x decreases. This can be explained again by the fact that for a given Rayleigh number (i.e. a given value of K_1) an increase in K^* corresponds to a decrease in K_2 resulting in a weaker convection flow and heat transfer rate.

Conclusions

A study has been made of natural convection near a semi-infinite plate embedded in an anisotropic porous medium where the principal axes are non-coincident with the gravity vector. Within the framework of boundary-layer approximations similarity solutions are derived for the case of a plate heated isothermally or by a constant heat flux. The main features of the approximate analytical solution have been tested by a numerical solution of the full governing equations in the range $10^1 \leq R_H \leq 10^4$, $0.1 \leq K^* \leq 10$ and $0 \leq \theta \leq 90°$. The main conclusions of the present analysis are:

(1) The convective flow along a vertical plate embedded in an anisotropic porous medium is considerably affected by both the permeability ratio K^* and inclination angle θ of the principal axes.

(2) When the orientation of the inclination angle is such that the principal axis with higher permeability is parallel to the plate the strength of the convective flow is maximum. This occurs for $K^* < 1$ when $\theta = 0°$ and $K^* > 1$ when $\theta = 90°$. For this situation the boundary-layer hypothesis is valid provided that the permeability along the plate is not considerably greater than that in the direction normal to it.

(3) For a fixed inclination θ the heat transfer is promoted, when compared with the isotropic situation ($K^* = 1$), as the permeability ratio K^* is made larger than unity and reduced when it is made smaller.

References

Bear, J. (1972), *Dynamics of Fluids in Porous Media*, Dover Publications.

Bejan, A. and Poulikakos, D. (1984), "The non-Darcy regime for vertical boundary-layer natural convection in a porous medium", *Int. J. Heat Mass Transfer,* Vol. 27, pp. 717-22.

Castinel, G. and Combarnous, M. (1974), "Critère d'apparition de la convection naturelle dans une couche poreuse anisotrope", *C.R. Hebd. Seanc. Acad. Sci.*, Paris B, B278, pp. 701-4.

Cheng, P. (1977), "Constant surface heat flux solutions for porous layer flows", *Letters Heat Mass Transfer*, Vol. 4, pp. 119-27.

Cheng, P. (1978), "Heat transfer in geothermal systems", *Adv. Heat Transfer*, Vol. 14, pp. 1-105.

Cheng, P. and Minkowycz, W. J. (1977), "Free convection about a vertical flat plate embedded in a saturated porous medium with application to heat transfer from a dyke", *J. Geophys. Res.*, Vol. 82, pp. 2040-44.

Degan, G. and Vasseur, P. (1996), "Natural convection in a vertical slot filled with an anisotropic porous medium with oblique principal axes", *Numerical Heat Transfer*.

Degan, G., Vasseur, P. and Bilgen, E. (1995), "Convective heat transfer in a vertical anisotropic porous layer", *Int. J. Heat Mass Transfer*, Vol. 38, pp. 1975-87.

Dutta, P. and Seetharamu, K.N. (1987), "Effect of variable wall heat flux on free convection in a saturated porous medium", *Indian J. Technology*, Vol. 25, pp. 567-71.

Dutta, P. and Seetharamu, K.N. (1993), "Free convection in a saturated porous medium adjacent to a vertical impermeable wall subjected to a non-uniform heat flux", *Wärme-und-Stoffübertragung*, Vol. 28, pp. 27-32.

Ene, H.I. (1991), "Effects of anisotropy on the free convection from a vertical plate embedded in a porous medium", *Transport in Porous Media*, Vol. 6, pp. 183-94.

Ene, H.I. and Polisevski, D. (1987), *Thermal Flow in Porous Media*, Reidel, Dordrecht.

Epherre, J.F. (1975), "Critère d'apparition de la convection naturelle dans une couche poreuse anisotrope", *Rev. Gen. Thermique*, Vol. 168, p. 950.

Evans, G.H. and Plumb, O.A. (1978), "Natural convection from a vertical isothermal surface embedded in a saturated porous media", *ASME*, Paper 72-HT-85.

Hong, J.T., Tien, C.L. and Kaviany, M. (1985), "Non-Darcy effects on vertical-plate natural convection in a porous media with high porosities", *Int. J. Heat Mass Transfer*, Vol. 28, pp. 2149-57.

Hsu, C.T. and Cheng, P. (1985), "The Brinkman model for natural convection about a semi-infinite vertical flat plate in a porous medium", *Int. J. Heat Mass Transfer*, Vol. 28, pp. 663-97.

Ingham, D.B., Merkin, J.H. and Pop, I. (1982), "Flow past a suddenly cooled vertical flat surface in a saturated porous medium", *Int. J. Heat Mass Transfer*, Vol. 25, pp. 1916-19.

Johnson, C. and Cheng, P. (1978), "Possible similarity solutions for free convection boundary layers adjacent to flat plates in porous media", *Int. J. Heat Mass Transfer*, Vol. 21, pp. 709-18.

Kaviany, M. and Mittal, M. (1987), "Natural convection heat transfer from a vertical plate to high permeability porous media: an experiment and an approximate solution", *Int. J. Heat Mass Transfer*, Vol. 30, pp. 967-77.

Kimura, S., Masuda, Y. and Kazuo Hayashi, T. (1993), "Natural convection in an anisotropic porous medium heated from the side (effects of anisotropic properties of porous matrix", *Heat Transfer Japanese Research*, Vol. 22, pp. 139-53.

Kvernvold, O. and Tyvand, P.A. (1979), "Nonlinear thermal convection in anisotropic porous media", *J. Fluid Mech.*, Vol. 90, pp. 609-24.

Mahajan, R.L. and Angirasa, D. (1993), "Combined heat and mass transfer by natural convection with opposing buoyancies", *J. Heat Transfer*, Vol. 115, pp. 606-12.

Nakayama, A. and Koyama, H. (1987), "An integral method for free convection from a vertical heated surface in a thermally stratified porous medium", *Wärme-und-Stoffübertragung*, Vol. 21, pp. 297-300.

Ni, J. and Beckermann, C. (1991), "Natural convection in a vertical enclosure filled with anisotropic porous media", *J. Heat Transfer*, Vol. 113, pp. 1033-7.

Nilsen, T. and Storesletten, L. (1990), "An analytical study on natural convection in isotropic and anisotropic porous channels", *J. Heat Transfer*, Vol. 112, pp. 396-401.

Plumb, O.A. and Huenefeld, J.C. (1981), "Non-Darcy natural convection from heated surfaces in a saturated porous media", *Int. J. Heat Mass Transfer*, Vol. 24, pp. 765-78.

Rajamani, R., Srinivas, C. and Seetharamu, K.N. (1990), "Finite element analysis of convective heat transfer in porous media", *Int. J. Num. Methods in Fluids*, Vol. 11, pp. 331-9.

Roache, P. J. (1982), *Computational Fluid Dynamic*s, Hermosa, Albuquerque, NM.

Seetharamu, K.N. and Dutta, P. (1990), "Free convection in a saturated porous medium adjacent to a non-isothermal vertical impermeable wall", *Wärme-und-Stoffübertragung*, Vol. 25, pp. 9-15.

Seetharamu, K.N., Satya Sai, B.V K., Aswatha Narayama, P.A. and Reddy, J.N. (1994), "Non-Darcy natural convection in porous cavity with constant heat flux on one vertical wall", *Proceedings, Int. Heat Transfer Conf.*, Brighton, August, Vol. 7, 16-NC-28.

Yücel, C., Hasnaoui, M., Robillard, L. and Bilgen, E. (1993), "Mixed convection heat transfer in open ended inclined channels with discrete isothermal heating", *Numerical Heat Transfer*, Vol. 24, pp. 109-26.

Zhang, X. (1993), "Convective heat transfer in a vertical porous layer with anisotropic permeability", *Proceedings 14th Canadian Congress of Applied Mechanics*, Vol. 2, pp. 579-80.